



## Article

# Laser-Induced Damage Threshold of Nonlinear GaSe and GaSe:In Crystals upon Exposure to Pulsed Radiation at a Wavelength of 2.1 $\mu\text{m}$

Chongqiang Zhu <sup>1</sup>, Victor Dyomin <sup>2</sup>, Nikolay Yudin <sup>2,3,4,\*</sup>, Oleg Antipov <sup>5,6,7</sup>, Galina Verozubova <sup>3</sup>, Ilya Eranov <sup>5,7</sup>, Mikhail Zinoviev <sup>2,3,4</sup> , Sergey Podzyvalov <sup>2,3,4</sup> , Yelena Zhuravlyova <sup>2</sup>, Yelena Slyunko <sup>2,3</sup> and Chunhui Yang <sup>8,\*</sup>

- <sup>1</sup> MIIT Key Laboratory of Critical Materials Technology for New Energy Conversion and Storage, School of Chemistry and Chemical Engineering, Harbin Institute of Technology, Harbin 150001, China; zcq90@hit.edu.cn
  - <sup>2</sup> Laboratory for Radiophysical and Optical Methods of Environmental Studies, National Research Tomsk State University, 634050 Tomsk, Russia; dyomin@mail.tsu.ru (V.D.); muxa9229@gmail.com (M.Z.); cginen@yandex.ru (S.P.); lenazhura@mail.ru (Y.Z.); elenohka266@mail.ru (Y.S.)
  - <sup>3</sup> LOC LLC., 634050 Tomsk, Russia; galina.veroz@mail.ru
  - <sup>4</sup> V.E. Zuev Institute of Atmospheric Optics SB RAS, 634055 Tomsk, Russia
  - <sup>5</sup> Institute of Applied Physics of the Russian Academy of Sciences, 46 Ulyanov St., 603950 Nizhny Novgorod, Russia; antipov@ipfran.ru (O.A.); 72ilya305@mail.ru (I.E.)
  - <sup>6</sup> Higher School of General and Applied Physics, Nizhny Novgorod State University, 26 Gagarin Av., 603950 Nizhny Novgorod, Russia
  - <sup>7</sup> Laboratory of Functional Materials, Novosibirsk State University, 630090 Novosibirsk, Russia
  - <sup>8</sup> State Key Laboratory of Urban Water Resource and Environment, School of Chemistry and Chemical Engineering, Harbin Institute of Technology, Harbin 150001, China
- \* Correspondence: rach3@yandex.ru (N.Y.); yangchh@hit.edu.cn (C.Y.)



**Citation:** Zhu, C.; Dyomin, V.; Yudin, N.; Antipov, O.; Verozubova, G.; Eranov, I.; Zinoviev, M.; Podzyvalov, S.; Zhuravlyova, Y.; Slyunko, Y.; et al. Laser-Induced Damage Threshold of Nonlinear GaSe and GaSe:In Crystals upon Exposure to Pulsed Radiation at a Wavelength of 2.1  $\mu\text{m}$ . *Appl. Sci.* **2021**, *11*, 1208. <https://doi.org/10.3390/app11031208>

Academic Editor: Domenico de Ceglia

Received: 24 November 2020

Accepted: 26 January 2021

Published: 28 January 2021

**Publisher's Note:** MDPI stays neutral with regard to jurisdictional claims in published maps and institutional affiliations.



**Copyright:** © 2021 by the authors. Licensee MDPI, Basel, Switzerland. This article is an open access article distributed under the terms and conditions of the Creative Commons Attribution (CC BY) license (<https://creativecommons.org/licenses/by/4.0/>).

**Abstract:** The paper defined the laser-induced damage threshold from the fluence and the peak power of GaSe and GaSe:In single crystals upon exposure to nanosecond radiation in the two micron range and assessed the influence of test radiation energy parameters (pulse repetition rate, pulse duration) on the damage threshold. Laser-induced damage threshold was determined with the parameters of the incident radiation close to the pump radiation parameters of promising dual-wavelength optical parametric oscillators (effective pump sources for THz difference frequency oscillators): wavelength was  $\approx 2.1 \mu\text{m}$ ; pulse repetition rates were 10, 12, 14, and 20 kHz; and pulse durations were 15, 18, 20, and 22 ns. The obtained results made it possible to conclude that the value of GaSe damage threshold at a wavelength of 2.091  $\mu\text{m}$  of the incident radiation was influenced by the accumulation effects (the damage threshold decreased as the pulse repetition rate increased). The accumulation effects were more significant in the case of the In-doped sample, since a more significant decrease in the damage threshold was observed with increasing frequency in terms of the peak power and the fluence.

**Keywords:** laser-induced damage threshold; GaSe; nonlinear crystals

## 1. Introduction

Generation of pulsed nanosecond THz radiation in the frequency range of 0.3–30 THz at a difference frequency with an average power of  $\approx 1$ –10 mW is an intensively developing area of laser technology and nonlinear optics [1,2]. Effective parametric generation at the difference frequency requires the use of nonlinear crystals with high optical transparency at all wavelengths—pumping, signal, and idler waves; a large second-order nonlinear susceptibility; high laser-induced damage threshold (LIDT); and good spatial homogeneity. The negative uniaxial GaSe crystal is one of the most famous and demanded nonlinear crystals in terms of its characteristics among the extensive variety of nonlinear optical crystals for oscillating THz radiation [1]. The transparency is in the range of 0.65–18  $\mu\text{m}$ . The absorption coefficient of this single crystal amounts to  $\approx 0.1 \text{ cm}^{-1}$  at a wavelength of

$\approx 2 \mu\text{m}$  [3], and, alongside  $\text{ZnGeP}_2$ , it is characterized by the lowest absorption among all nonlinear crystals in the THz spectral range (90–1000  $\mu\text{m}$ ) [4]. The material has high birefringence, nonlinear susceptibility of GaSe is  $\approx 54 \text{ pm/V}$  [3], and high thermal conductivity reaching  $\approx 16 \text{ W m}^{-1} \text{ K}^{-1}$  (which allows for phase matching to be carried out over a wide range). GaSe has a layered structure along the C axis. Weak Van der Waals forces occur between the layers, while strong covalent bonds and an ionic component are inside the layers. Such structure makes the material soft with the Mohs hardness [3] of  $\approx 1$ . This is the main disadvantage of GaSe. GaSe samples are difficult to cut at various angles to the C axis and polish. Therefore, in almost all known devices, GaSe crystals are made by splitting, and the working surfaces are parallel to the c-face.

The use of a dual-wavelength degenerate optical parametric oscillator (OPO) based on a nonlinear KTP crystal with intracavity pumping by  $\text{Nd}^{3+}$ :YAG laser as a pumping source is one of the most effective ways to generate powerful tunable THz radiation at a difference frequency in nonlinear crystals including GaSe [5]. These sources are capable of generating powerful tunable dual-wavelength radiation with an orthogonal polarization near the degeneration point of  $2.12 \mu\text{m}$  with an average power of  $\approx 10 \text{ W}$  and a pulse power of  $\approx 100 \text{ KW}$  at a pulse repetition rate of  $\approx 1\text{--}10 \text{ kHz}$  and a pulse duration of  $\approx 10\text{--}20 \text{ ns}$  [6–8]. The most efficient nonlinear crystals for generating THz radiation, such as GaSe and  $\text{ZnGeP}_2$ , have minimum absorption in this wavelength range, which compares favorably this pump source with dual-wavelength tunable (or with a discrete set of wavelengths) systems operating in the spectral region of  $\approx 1 \mu\text{m}$  or  $\approx 10 \text{ microns}$ .

The problem of GaSe damage by laser radiation at the wavelengths of  $1\text{--}10 \mu\text{m}$  was covered in several previously published works [9–12]. In particular, these works described that in terms of the intensity of the acting beam at a wavelength of  $9.55 \mu\text{m}$ , the GaSe LIDT was  $121 \text{ MW/cm}^2$  with pulse duration of  $\approx 30 \text{ ns}$  and the repetition rate of  $1 \text{ Hz}$  [9].

In Reference [12], GaSe LIDT was studied when exposed to radiation from the following lasers: Ti:Sapphire laser ( $\lambda$ -800 nm, pulse duration—100 fs); frequency-tunable optical parametric amplifier ( $\lambda$ -1.1–2.9  $\mu\text{m}$ , pulse duration—60–90 fs); TEA (Transversely Excited Atmospheric)  $\text{CO}_2$  laser ( $\lambda$ -10.6  $\mu\text{m}$ , pulse duration—50 ns);  $\text{Er}^{3+}$ :YSGG laser ( $\lambda$ -2.79  $\mu\text{m}$ , pulse duration—250 ns). It was shown that when GaSe is exposed to femtosecond radiation, the local microdefects and the induced field effects—for example, dissociation of GaSe and multiphoton absorption—have strong impact on LIDT. It is also noted that under the influence of pulse nanosecond laser radiation, the thermal effects have a considerable influence on GaSe LIDT.

However, there is currently no sufficient information on LIDT of a nonlinear GaSe crystal when exposed to laser radiation in a repetitively pulsed mode at pulse repetition rates of  $\approx 10 \text{ kHz}$  and higher at exposure wavelengths of  $\approx 2.1 \mu\text{m}$  and pulse durations of  $\approx 20 \text{ ns}$  and lower. This hinders the progress in generating THz radiation at a difference frequency in nonlinear GaSe crystals and does not allow for determination of the optimal energy parameters of pump radiation for the conditions of the most efficient generation of THz irradiation. Moreover, there are insufficient data on the effect of various technological processes on GaSe damage threshold in the wavelength range of  $\approx 2.1 \mu\text{m}$ , including doping of crystals with chemical elements such as In.

The purpose of the paper is to determine LIDT of GaSe and GaSe:In single crystals upon exposure to nanosecond radiation in the two-micron range and to assess the influence of pump radiation energy parameters (pulse repetition rate, pulse duration) on the damage threshold. The obtained data are proposed to be used for the subsequent optimization of the pump radiation energy parameters (in the wavelength range of  $\approx 2.1 \mu\text{m}$ ) of THz sources based on difference frequency generation using GaSe and GaSe:In crystals.

## 2. Test Samples and Research Technique

Two crystals GaSe (sample no. 1) and GaSe:In (sample no. 2) produced by Harbin Institute of Technology, China, were used as the test samples. Sample no. 2 was doped with In. The thickness of sample no. 1 was  $3.1 \text{ mm}$ , the sample aperture was  $8 \times 5 \text{ mm}^2$

(rectangle), the thickness of sample No. 2 was 4.49 mm, and the sample aperture was  $5 \times 7 \text{ mm}^2$ . The working surfaces of the samples were orthogonal to the optical axis of the crystal.

Se (6N) and Ga (6N) were used for GaSe synthesis. They were purified firstly in Aqua Regia and then carefully washed in distilled water fused silica ampules, and pyrolytic boron nitride (PBN) loads and crucibles were used for synthesis and growth. The ampules with substances were pumped down  $10^{-5} \text{ mm Hg}$ . The single-temperature method was applied for synthesis. GaSe crystals with a diameter of 30 and 40 mm were grown by vertical Bridgeman (VB) method. The high-temperature zone was  $1075 \text{ }^\circ\text{C}$  and the low-temperature zone was  $920 \text{ }^\circ\text{C}$ . The temperature gradient was  $4 \text{ deg/cm}$  and the pulling rate was  $0.5 \text{ mm/h}$ .

The surface roughness of both samples was identical and was determined using a Bruker Dimension Edge atomic force microscope (AFM). AFM scanning of the samples was carried out on the area of  $10 \times 10 \text{ }\mu\text{m}$  at room temperature. The result of determining the surface roughness of sample no. 1 is shown in Figure 1.

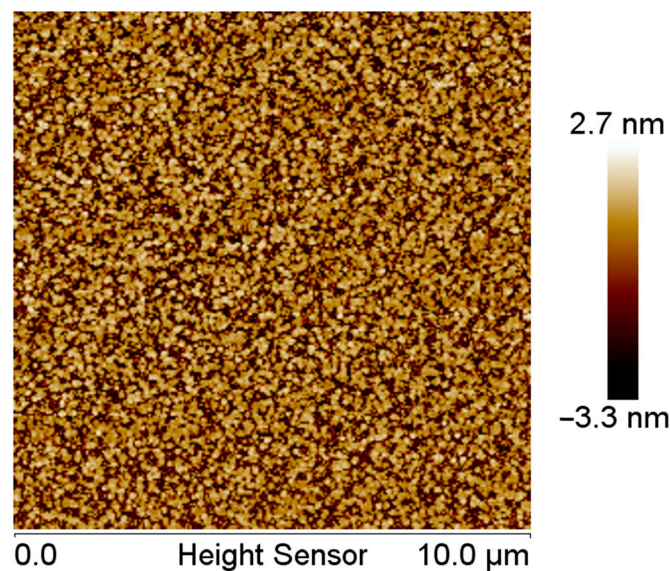


**Figure 1.** Example of the roughness profile of the test sample no. 1 measured using a Bruker Dimension Edge atomic force microscope (AFM).

Figure 1 shows that the maximum difference in height and depth of inhomogeneities on the surface of the samples was 6 nm.

A  $\text{Ho}^{3+}$ :YAG laser developed at the IAP RAS was used as a source of laser radiation. Lasing was carried out at a wavelength of  $2.091 \text{ }\mu\text{m}$  (close to the radiation wavelength of  $2.12 \text{ }\mu\text{m}$  produced in the process of degenerate parametric generation based on a KTP crystal) [13]. Lasing was carried out in the active Q-switching mode using an acousto-optic modulator with pulse duration  $\tau$  equal to 15, 18, 20, or 23 ns, depending on the pulse repetition rate  $f$  equal to 10, 12, 14, or 20 kHz, respectively. To avoid changes in the pulse duration and the intensity distribution in the cross section of the generated beam, we pumped the  $\text{Ho}^{3+}$ :YAG laser with a thulium fiber laser with a fixed average power of 50 W. The maximum average radiation power generated by the  $\text{Ho}^{3+}$ :YAG laser was 30 W in a linearly polarized high-quality Gaussian beam ( $M^2$  was less than 1.2). The scheme of the test setup is shown in Figure 2. The stand consisted of the following elements: 1— $\text{Ho}^{3+}$ :YAG laser; F.I.—Faraday optical isolator; A—attenuator, which was used to adjust the power level (consisted of a half-wave plate and a polarizing mirror M1 with high transmittance in p-polarization and high reflection in s-polarization); T—two-lens Galilean telescope focusing radiation on the test samples; Sample—sample under study fixed in a holder, adjusted in angle and transverse coordinates; P.M.—power meter. The average radiation

power  $P_a$  was measured using a power meter immediately before installation of the test samples. The studied plates were deviated from the position corresponding to normal incidence by 3–5° to prevent the reflected radiation from entering the laser exit window.

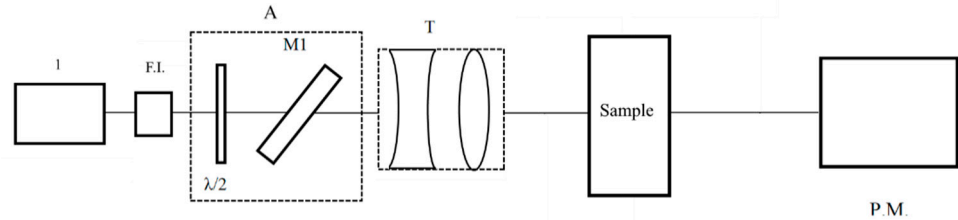


**Figure 2.** Schematic layout of the test stand.

The diameter of the laser beam at the  $1/e^2$  level in the plane corresponding to the entrance aperture of the tested plate was measured by the Foucault knife-edge test according to the technique described in [14,15]. The diameter of the radiation beam measured in the knife plane (sample installation) was  $d = (280 \pm 10 \mu\text{m})$  at the  $1/e^2$  level. Figure 3 shows the intensity distribution over the laser beam diameter. According to the international standard International Organization for Standardization (ISO) 21254, the effective area of the Gaussian beam is  $S = \pi d^2/4$  [15]. The laser fluence was determined by Equation (1):

$$W = 8 P_a / (f \pi d^2). \quad (1)$$

The laser power density was determined by Equation (2):

$$I = 8 P_a / (f \tau \pi d^2). \quad (2)$$

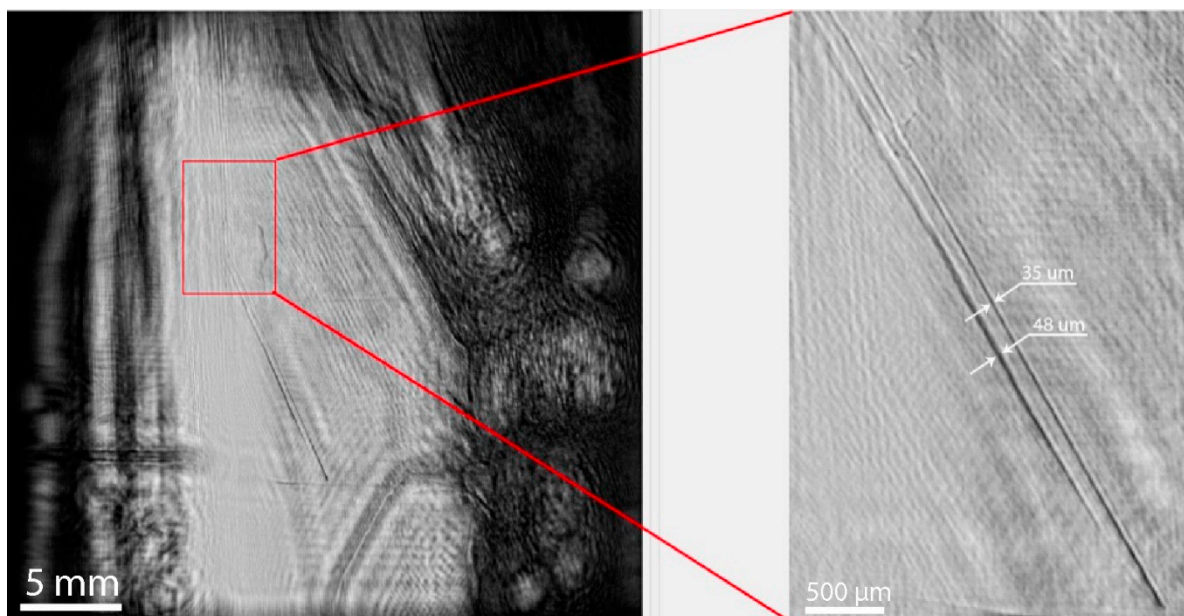


**Figure 3.** Reconstructed holographic image of GaSe (sample no. 1) in the best focus plane containing images of microcracks (left) and their magnified images (right).

### 3. Results

There are two main mechanisms of optical damage of nonlinear crystals accompanied by accumulative effects. The first is caused by thermal heating of the material when absorbing laser radiation with volumetric defects. The volumetric defects, as well as



the defect-matrix medium boundary, may have an absorption coefficient significantly higher than the matrix medium, and may cause optical damage being heated to the melting point when absorbing laser radiation. Thus, at a high frequency of laser radiation pulses, the absorption heating may exceed the heat removal from the defect due to the thermal conductivity of the material and cause an “accumulative effect”, leading to material breakdown. The second proposed mechanism is nonlinear absorption associated with the transition of charge carriers to impurity levels for example, formed by point defects, under the influence of laser radiation. The point defects caused by the incorporation of impurity atoms into the crystal lattice or the formation of vacancies and the substitution of atoms of the original semiconductor components may be the sources of impurity levels in the semiconductor. Due to the transition of free charge carriers to impurity levels the absorption may increase many times as the intensity of laser radiation increases. This may result in the material being heated to temperatures above the melting point and, as a result, to the optical damage.

To assess the effect of volumetric defects on the optical damage threshold, we determined the presence or absence, as well as the geometry of volumetric defects, in all tested samples through using the digital holography. To assess the effect of point defects on the optical damage threshold, we measured the absorption at the wavelength of exposure radiation (since the presence of point defects leads to the formation of impurity levels in the band gap, which may significantly affect the absorption coefficient at the exposure wavelength).

The study of LIDT was preceded by recording the digital holograms of the test samples using a 1.064  $\mu\text{m}$  digital holographic camera (DHC) manufactured by LLC Laboratory of Optical Crystals. Computer reconstruction of holographic images was carried out from the recorded holograms in order to determine internal inhomogeneities and volumetric defects. The limiting resolution of the method was 15  $\mu\text{m}$ . A detailed description of the digital holography technique and a description of the setup are given in [16,17].

According to the results of the holographic test, the GaSe (sample no. 1) did not contain any inclusions and volumetric defects except for the microcracks shown in Figure 3. However, volumetric inclusions with a size of  $\approx 300 \mu\text{m}$  were found in GaSe:In (sample no. 2) (Figure 4).

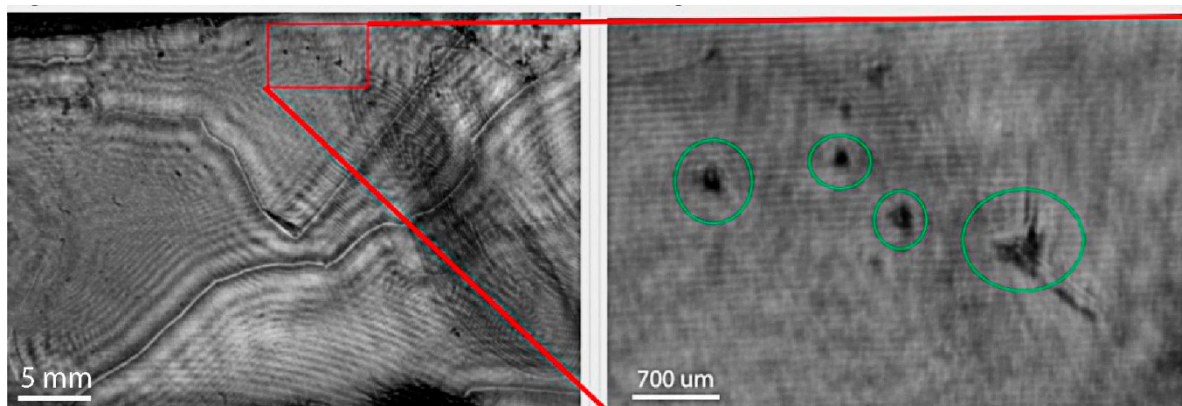


**Figure 4.** Reconstructed holographic image of GaSe:In (sample no. 2) in the best focus plane containing images of inclusions (left) and magnified images of regions containing inhomogeneities (right).

Then, the transmittance of both samples was measured, and the absorption was calculated, taking into account multiple reflections from the plane-parallel faces of the plates at a wavelength of 2.091  $\mu\text{m}$ . The beam reflection losses in GaSe sample were calculated using dispersion equations for refractive index of ordinary and extraordinary waves obtained in the study [18]. The following results presented in Table 1 were obtained by determining the transmittance at a wavelength of 2.091  $\mu\text{m}$  and calculating the absorption.

**Table 1.** Absorption coefficient of the samples at a wavelength of the Ho<sup>3+</sup>:YAG laser—2.091 μm.

Sample	T, %	d, mm	α, cm <sup>-1</sup>
GaSe (No. 1)	0.6	3.1	0.17
GaSe:In (No. 2)	0.47	4.49	0.39

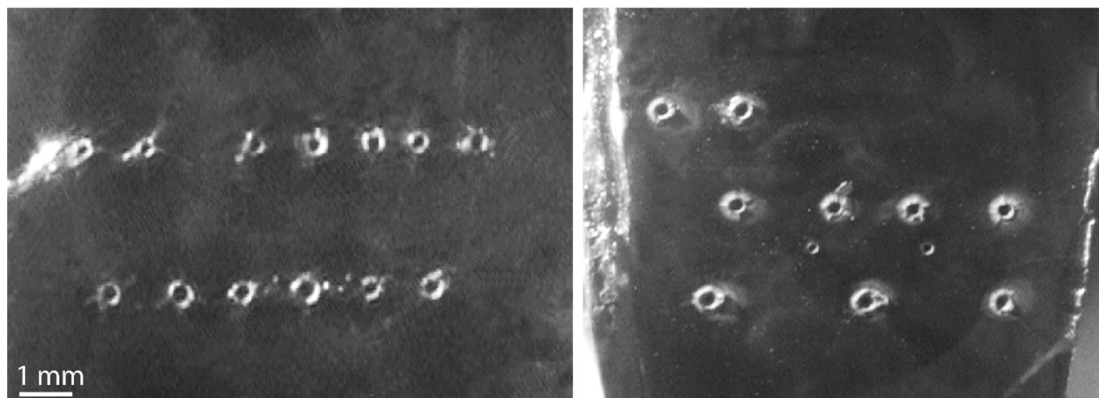
The R-on-1 method [19] was used to determine LIDT since the aperture of the samples under study was limited in the given experiment. The key principle of the R-on-1 technique is that each separate region of the crystal is exposed to laser radiation with a gradual increase in the laser radiation intensity until the occurrence of an optical damage or a given value of the energy density is reached [20]. The testing of samples for LIDT using the R-on-1 technique included the exposure of the studied plate to pulsed laser radiation with a fixed fluence level during the exposure time of 1 s. Further, the fluence was increased with a step of 0.1 J/cm<sup>2</sup>. The fact of the optical damage was established by the appearance of a glow in the area of exposure and a decrease in radiation transmission, as well as upon appearance of a damage on one of the crystal surfaces. Then, the sample was moved 0.7 mm in height or horizontally using a two-coordinate movement, and the experiment was repeated. The measurements were taken five times in order to obtain statistical data. Figure 5 shows the surfaces of GaSe samples with traces of the optical damage. The obtained experimental data served as a basis for constructing a graph of the cumulative probability of an optical damage depending on the fluence of the laser action. The point with the maximum fluence at which the damage occurred was assigned the probability  $P_D = (5/5) = 1$ ; the point with the lower fluence value was assigned the probability  $P_D = (4/5) = 0.8$ , etc.; and the point with the minimum fluence value was assigned the probability— $P_D = (1/5) = 0.2$ . Then, the experimental data were linearly approximated to the zero value of the optical damage probability. The fluence value of the incident radiation corresponding to the zero probability of the optical damage  $P_D = 0$  was taken as the damage threshold  $W_{0d}$ . The average value of the optical damage fluence was also calculated by using Equations (3)–(6):

$$W_{av} = \frac{\sum W_i n_i}{N}, \quad (3)$$

and mean square error:

$$\Delta W_{av}^2 = \frac{\sum (W_{av} - W_i)^2 n_i}{N(N - 1)}, \quad (4)$$

where  $N$ —total number of damaged sections,  $W_{av}$ —average value of the damage threshold,  $W_i$ —value of the damage threshold at one of  $N$  points, and  $n_i$ —number of points with the damage threshold  $W_i$ .

**Figure 5.** Surface of studied GaSe samples no. 1 (left) and no. 2 (right) upon laser radiation exposure.

The following formula was used to find the confidence interval for LIDT ( $W_D$ ):

$$W_D = W_{av} \pm k < \Delta W_{av}^2 >^{1/2}, \tag{5}$$

where  $k$ —Student’s coefficient. Student’s  $t$ -distribution was used for the confidence probability Equation (5) [20,21]:

$$F(k, N) = \frac{\Gamma(N/2)}{\sqrt{\pi(N-1)}\Gamma[(N-1)/2]} \int_{-k}^k \left(1 + \frac{z^2}{N-1}\right)^{-N/2} dz, \tag{6}$$

where  $\Gamma$ —gamma function.

After the absorption of the samples was determined, LIDT values were obtained for each sample in terms of the fluence  $W_{0d}^E$  and the peak power  $W_{0d}^P$  of laser radiation at the probability of laser-influenced damage  $P_D = 0$ , according to the method described above. The average fluence  $W_{av}^E$  and the peak power  $W_{av}^P$  of the test radiation were found using Equations (1)–(5), at which the laser-induced damage of the sample took place. The confidence interval of LIDT in terms of the fluence  $W_D^E$  and the peak power  $W_D^P$  was also obtained. The experimental results are shown in Figures 6 and 7 and Table 2.

**Table 2.** Laser-induced damage threshold (LIDT) results for GaSe: the values of fluence  $W_{0d}^E$  and peak power  $W_{0d}^P$  with LIDT probability equal to 0, the values of fluence  $W_{1d}^E$  and peak power  $W_{1d}^P$  with LIDT probability equal to 1, the average value of fluence  $W_D^E$  and peak power  $W_D^P$  taking into account the measurement error; Student’s coefficient  $k$  at confidence probability—0.95, standard deviation— $\sqrt{s^2}$ , number of measurements— $N$ .

Sample	N	f, kHz	$\tau$ , ns	$\Delta W_{av}^2$	k	$W_D^E$ , J/cm <sup>2</sup>	$W_{0d}^E$ , J/cm <sup>2</sup>	$W_{1d}^E$ , J/cm <sup>2</sup>	$W_D^P$ , MW/cm <sup>2</sup>	$W_{0d}^P$ , MW/cm <sup>2</sup>	$W_{1d}^P$ , MW/cm <sup>2</sup>
GaSe (no. 1)	5	10	15	0.09	2.8	(2.8 ± 0.3)	2.4	3.1	(95 ± 28)	82	103
	5	12	18	0.08	2.8	(3.6 ± 0.2)	2.4	4.4	(101 ± 20)	69	121
	5	14	20	0.001	2.8	(2.561 ± 0.003)	2.4	2.6	(66.5 ± 0.4)	64	67
	5	20	23	0.01	2.8	(3.53 ± 0.04)	3.01	3.9	(50 ± 21)	43	55
GaSe:In (no. 2)	5	10	15	0.02	2.8	(4.69 ± 0.06)	4.1	5	(157 ± 59)	137	169
	4	12	18	0.03	3.2	(4.06 ± 0.09)	3.35	4.5	(113 ± 28)	93	126
	5	14	20	0.08	2.8	(3.1 ± 0.2)	2.7	3.4	(86.3 ± 0.8)	83	87
	5	20	23	0.08	2.8	(2.9 ± 0.2)	2.2	3.2	(42 ± 22)	31	45

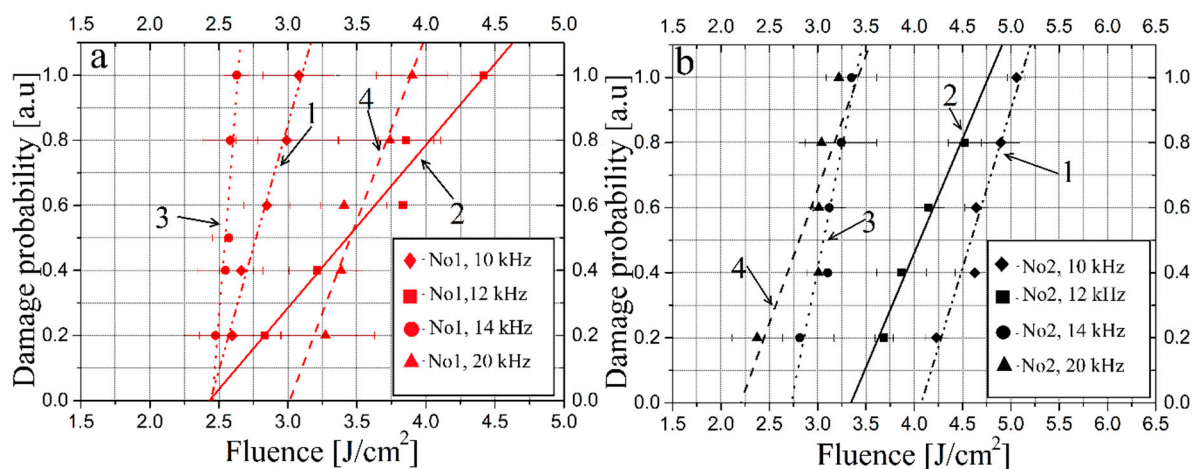


**Figure 6.** (a) Dependences of the sample no. 1 (GaSe) damage probability on the fluence of the acting radiation (exposure time—1 s): 1—at a pulse repetition rate of 10 kHz; 2—at a pulse repetition rate of 12 kHz; 3—at a pulse repetition rate of 14 kHz; 4—at a pulse repetition rate of 20 kHz. (b) Dependences of the sample no. 2 (GaSe:In) damage probability on the fluence of the acting radiation (exposure time—1 s): 1—at a pulse repetition rate of 10 kHz; 2—at a pulse repetition rate of 12 kHz; 3—at a pulse repetition rate of 14 kHz; 4—at a pulse repetition rate of 20 kHz.

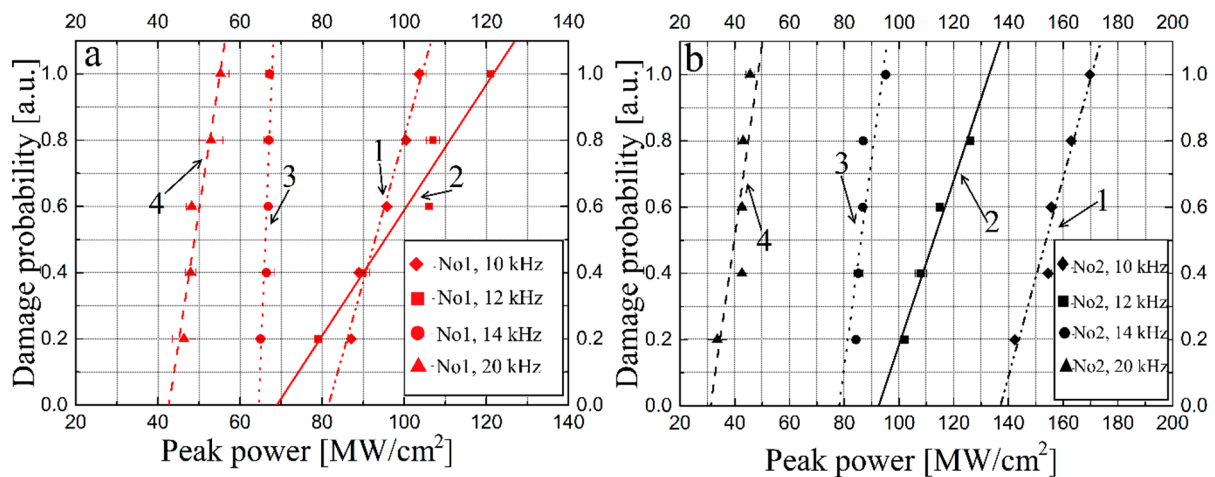


**Figure 7.** (a) Dependences of the sample no. 1 (GaSe) damage probability on the damage peak power (exposure time—1 s): 1—at a pulse repetition rate of 10 kHz; 2—at a pulse repetition rate of 12 kHz; 3—at a pulse repetition rate of 14 kHz; 4—at a pulse repetition rate of 20 kHz. (b) Dependences of the sample no. 2 (GaSe:In) damage probability on the damage peak power (exposure time—1 s): 1—at a pulse repetition rate of 10 kHz; 2—at a pulse repetition rate of 12 kHz; 3—at a pulse repetition rate of 14 kHz; 4—at a pulse repetition rate of 20 kHz.

#### 4. Discussion

The results of the study indicate that the damage threshold of In-doped GaSe single crystal (sample no. 2) and undoped single crystal (sample no. 1) had different dependences on the pulse repetition rate of the testing laser radiation. A more significant decrease in LIDT with an increase in the pulse repetition rate was observed in the In-doped sample, as compared to the undoped one. In terms of the fluence, the damage threshold of sample no. 1 did not actually change as the pulse repetition rate increased, but the fluence threshold decreased with an increase in the repetition rate of radiation pulses. From the results presented in Figures 6 and 7, as well as in Table 2, it can be seen that there was no correlation between LIDT and the intrinsic absorption of the sample. At the same time, the results obtained using digital holography methods (Figures 3 and 4), as well as the results presented in Figures 6 and 7 and Table 2 indicate that the presence of volumetric defects in the GaSe:In-doped single crystal enhanced the accumulative effects compared to the undoped crystal (in which the digital holography did not detect any volumetric defects).

Thus, the obtained results made it possible to conclude that the value of GaSe damage threshold at a test radiation wavelength of 2.091  $\mu\text{m}$  was influenced by accumulation effects (the damage threshold decreased as the pulse repetition rate and the pulse duration increased). The accumulation effects were more significant in the In-doped sample, since an increase in the frequency led to a more significant decrease in the damage threshold in terms of fluence and peak power, as compared to the undoped sample (for which the damage threshold in the fluence did not actually change with increasing frequency). The results obtained during the study indicate that doping with In enhanced the accumulation effect, which manifested itself in a decrease in the damage threshold with increasing frequency. The experimental results indicated that GaSe LIDT depends on both the fluence and the peak power of the test laser radiation.

The results of this work confirm the conclusions obtained in Reference [12] on the significant influence of thermal effects on GaSe LIDT when exposed to pulsed nanosecond laser radiation, the role of which increases with the increase of pulse duration and laser pulse repetition rate.

#### 5. Conclusions

The digital holography method revealed defects with a characteristic size of  $\approx 300 \mu\text{m}$  in the volume of In-doped GaSe. LIDT was determined from the fluence and the peak



power of GaSe (sample no. 1) and GaSe:In (sample no. 2) crystals with the parameters of the incident radiation close to the pump radiation parameters of promising dual-wavelength optical parametric oscillators (effective pump sources for THz difference frequency oscillators): wavelength was  $\approx 2.1 \mu\text{m}$ , pulse repetition rate was 10–20 kHz, pulse duration was 15–22 ns. The damage threshold of GaSe crystal (sample no. 1) at a pulse repetition rate of 10 kHz was  $W_{0d}^E = 2.4 \text{ J/cm}^2$  in terms of the fluence of the acting laser radiation, and  $W_{0d}^P = 95 \text{ MW/cm}^2$  in terms of the peak power at a pulse repetition rate of 20 kHz  $W_{0d}^E = 3.01 \text{ J/cm}^2$ ,  $W_{0d}^P = 50 \text{ MW/cm}^2$ . The damage threshold of GaSe:In crystal (sample no. 2) at a pulse repetition rate of 10 kHz was  $W_{0d}^E = 4.1 \text{ J/cm}^2$  in terms of the fluence of the acting laser radiation, and  $W_{0d}^P = 157 \text{ MW/cm}^2$  in terms of the peak power at a pulse repetition rate of 20 kHz  $W_{0d}^E = 2.2 \text{ J/cm}^2$ ,  $W_{0d}^P = 42 \text{ MW/cm}^2$ .

The obtained results allow for the conclusion that the value of GaSe damage threshold at a wavelength of  $2.091 \mu\text{m}$  of the incident radiation was influenced by the accumulation effects (the damage threshold decreased as the pulse repetition rate increased). The accumulation effects were more significant in the case of the In-doped sample, since a more significant decrease in the damage threshold was observed with increasing frequency in terms of the peak power and the fluence. The presence of volumetric defects reaching geometric dimensions of  $\approx 300 \mu\text{m}$  in the GaSe:In sample seemed to enhance the accumulative effect. The results of this work confirm the conclusions obtained in [12] on the significant influence of thermal effects on GaSe LIDT when exposed to pulsed nanosecond laser radiation, the role of which increased with the increase of pulse duration and laser pulse repetition rate. The influence of thermal effects was enhanced by the presence of volumetric defects in the samples.

The obtained results will be useful in the design and development of THz radiation oscillators based on GaSe crystals with dual-wavelength pumping by radiation in the region of  $\approx 2.1 \mu\text{m}$ . The obtained results provide an analytical basis for determining the energy parameters of the pump radiation in order to improve energy characteristics of the THz radiation generated in GaSe and the stability of the system in the continuous mode.

**Author Contributions:** Conceptualization, G.V., O.A., N.Y., C.Y.; methodology, O.A., N.Y., M.Z., V.D.; software, Y.Z., Y.S.; validation, C.Z., C.Y.; formal analysis, C.Z., S.P.; investigation, N.Y., C.Z., O.A., I.E.; resources, C.Y., O.A., V.D.; data curation, V.D., O.A.; writing—original draft preparation, N.Y., M.Z., V.D., O.A.; writing—review and editing, O.A., V.D.; visualization, G.V., I.E.; supervision, O.A., V.D.; project administration, V.D., O.A., C.Y.; funding acquisition, V.D., O.A., C.Y. All authors have read and agreed to the published version of the manuscript.

**Funding:** This research was supported by Ministry of Science and Higher Education of the Russian Federation, project no. 0721-2020-0038.

**Institutional Review Board Statement:** Not applicable.

**Informed Consent Statement:** Not applicable.

**Data Availability Statement:** Not applicable.

**Conflicts of Interest:** The authors declare no conflict of interest.

## References

1. Kh, K.G. Terahertz generation by means of optical lasers. *Laser Phys. Lett.* **2008**, *5*, 559–576.
2. Creeden, D.; McCarthy, J.C.; Ketteridge, P.A.; Southward, T.; Schunemann, P.G.; Komiak, J.J.; Dove, W.; Chicklis, E.P. Compact Fiber-Pumped Terahertz Source Based on Difference Frequency Mixing in ZGP. *IEEE J. Sel. Top. Quantum Electron.* **2007**, *13*, 732–736. [[CrossRef](#)]
3. Dmitriev, V.G.; Gurzadyan, G.G.; Nikogosyan, D.N. *Handbook of Nonlinear Optical Crystals*; Springer: New York, NY, USA, 1999; p. 413.
4. Shi, W.; Ding, Y.J.; Schunemann, P.G. Coherent terahertz waves based on difference-frequency generation in an annealed zinc-germanium phosphide crystal: Improvements on tuning ranges and peak powers. *Opt. Commun.* **2004**, *233*, 183–189. [[CrossRef](#)]
5. Geng, Y.; Tan, L.; Yao, J. Compact and widely tunable terahertz source based on a dual-wavelength intracavity optical parametric oscillation. *Appl. Phys. B* **2010**, *99*, 181–185. [[CrossRef](#)]

6. Mei, J.; Zhong, K.; Wang, M.; Liu, Y.; Xu, D.; Shi, W.; Wang, Y.; Yao, J.; Norwood, R.A.; Eyghambarian, N.P. Widely-tunable high-repetition-rate terahertz generation in GaSe with a compact dual-wavelength KTP OPO around 2  $\mu\text{m}$ . *Opt. Express*. **2016**, *24*, 23368–23375. [[CrossRef](#)] [[PubMed](#)]
7. Yan, D.; Wang, Y.; Xu, D.; Liu, P.; Yan, C.; Shi, J.; Liu, H.; He, Y.; Tang, L.; Feng, J. High-average-power, high-repetition-rate tunable terahertz difference frequency generation with GaSe crystal pumped by 2  $\mu\text{m}$  dual-wavelength intracavity KTP optical parametric oscillator. *Photonics Res.* **2017**, *5*, 82–87. [[CrossRef](#)]
8. Sirotkin, A.A.; Yudin, N.N.; Dyomin, V.V.; Gribenyukov, A.I. Tunable THz-radiation in a ZnGeP<sub>2</sub> single crystal pumped by dual-wavelength degenerate optical parametric oscillator. *Laser Phys. Lett.* **2020**, *17*, 035402. [[CrossRef](#)]
9. Andreev, Y.M.; Badikov, V.V.; Voevodin, V.G.; Geiko, L.G.; Geiko, P.P.; Ivashchenko, M.V.; Karapuzikov, A.I.; Sherstov, I.V. Radiation resistance of nonlinear crystals at a wavelength of 9.55  $\mu\text{m}$ . *Quantum Electron.* **2001**, *31*, 1075–1078. [[CrossRef](#)]
10. Vodopyanov, K.L.; Kulevskii, L.A.; Voevodin, V.G.; Gribenyukov, A.I.; Allakhverdiev, K.R.; Kerimov, T.A. High efficiency middle IR parametric superradiance in ZnGeP<sub>2</sub> and GaSe crystals pumped by an erbium laser. *Opt. Commun.* **1991**, *83*, 322–326. [[CrossRef](#)]
11. Vodopyanov, K.L.; Voevodin, V.G. 2.8  $\mu\text{m}$  laser pumped type-I and type-II travelling-wave optical parametric generator in GaSe. *Opt. Commun.* **1995**, *114*, 333–335. [[CrossRef](#)]
12. Jin, G.; Ji-Jiang, X.; Lai-Ming, Z.; Fei, C.; Ke, J.; Alexeev, S.V.; Andreev, Y.M.; Kokh, K.A.; Lanskii, G.V.; Losev, V.F. GaSe damage threshold under IR pulse pumping. In Proceedings of the SPIE, XIX International Symposium on High-Power Laser Systems and Applications, Tomsk, Russia, 10–14 September 2012; Volume 8677, p. 86771E.
13. Antipov, O.L.; Kositsyn, R.I.; Eranov, I.D. 36W Q-switched Ho<sup>3+</sup>:YAG laser at 2097 nm pumped by a Tm fiber laser: Evaluation of different Ho<sup>3+</sup> doping concentrations. *Laser Phys. Lett.* **2017**, *14*, 015002. [[CrossRef](#)]
14. Yudin, N.N.; Zinovev, M.M.; Korsakov, V.S. Optical breakdown threshold of silver halide polycrystalline structures acted on by the pulsed radiation of a Ho:YAG laser. *J. Opt. Tech.* **2019**, *86*, 379–384. [[CrossRef](#)]
15. *Lasers and Laser-Related Equipment—Test Methods for Laser Beam Widths, Divergence Angles and Beam Propagation Ratios*; ISO 11146-1:2005; American National Standards Institute (ANSI): Washington, DC, USA, 2005.
16. Dyomin, V.; Gribenyukov, A.; Podzyvalov, S.; Yudin, N.; Zinoviev, M.; Polovtsev, I.; Davydova, A.; Olshukov, A. Application of Infrared Digital Holography for Characterization of Inhomogeneities and Voluminous Defects of Single Crystals on the Example of ZnGeP<sub>2</sub>. *Appl. Sci.* **2020**, *10*, 442. [[CrossRef](#)]
17. Dyomin, V.; Gribenyukov, A.; Davydova, A.; Zinoviev, M.; Olshukov, A.; Podzyvalov, S.; Polovtsev, I.; Yudin, N. Holography of particles for diagnostics tasks [Invited]. *Appl. Opt.* **2019**, *58*, G300–G310. [[CrossRef](#)] [[PubMed](#)]
18. Kato, K.; Tanno, F.; Umemura, N. Sellmeier and thermo-optic dispersion formulas for GaSe (Revisited). *Appl. Opt.* **2013**, *52*, 2325–2328. [[CrossRef](#)] [[PubMed](#)]
19. Lidaris LIDT Service. The R-on-1 Test. 2019. Available online: <http://lidaris.com/laserdamage-testing/> (accessed on 16 November 2020).
20. *Statistical Interpretation of Test Results—Estimation of the Mean—Confidence Interval*; ISO 2602:1980; American National Standards Institute (ANSI): Washington, DC, USA, 1980.
21. Fisher, R.A.; Rothamsted, M.A. Applications of “Student’s” Distribution. *Metron* **1995**, *5*, 90–104.